Detection of ultra-low oxygen concentration based on the fluorescence blinking dynamics of single molecules

Ruixiang Wu, Ruiyun Chen, Haitao Zhou, Yaqiang Qin, Guofeng Zhang, Chengbing Qin, Yan Gao, Yajun Gao, Liantuan Xiao, and Suotang Jia

Citation: Appl. Phys. Lett. **112**, 053101 (2018); doi: 10.1063/1.5005157
View online: https://doi.org/10.1063/1.5005157
View Table of Contents: http://aip.scitation.org/toc/apl/112/5
Published by the American Institute of Physics

Detection of ultra-low oxygen concentration based on the fluorescence blinking dynamics of single molecules

Ruixiang Wu,[1,2,3] Ruiyun Chen,[1,2,a)] Haitao Zhou,[1,2] Yaqiang Qin,[1,2] Guofeng Zhang,[1,2] Chengbing Qin,[1,2] Yan Gao,[1,2] Yajun Gao,[1,2] Liantuan Xiao,[1,2,b)] and Suotang Jia[1,2]
[1]*State Key Laboratory of Quantum Optics and Quantum Optics Devices, Institute of Laser Spectroscopy, Shanxi University, Taiyuan, Shanxi 030006, China*
[2]*Collaborative Innovation Center of Extreme Optics, Shanxi University, Taiyuan, Shanxi 030006, China*
[3]*College of Physics and Information Engineering, Shanxi Normal University, Linfen, Shanxi 041000, China*

(Received 18 September 2017; accepted 11 January 2018; published online 29 January 2018)

We present a sensitive method for detection of ultra-low oxygen concentrations based on the fluorescence blinking dynamics of single molecules. The relationship between the oxygen concentration and the fraction of time spent in the off-state, stemming from the population and depopulation of triplet states and radical cationic states, can be fitted with a two-site quenching model in the Stern-Volmer plot. The oxygen sensitivity is up to 43.42 kPa^{-1} in the oxygen partial pressure region as low as 0.01–0.25 kPa, which is seven times higher than that of the fluorescence intensity indicator. This method avoids the limitation of the sharp and non-ignorable fluctuations that occur during the measurement of fluorescence intensity, providing potential applications in the field of low oxygen-concentration monitoring in life science and industry. *Published by AIP Publishing.*
https://doi.org/10.1063/1.5005157

Oxygen, which undoubtedly belongs to one of the most important substances on the planet, is indispensable in many aspects of our daily lives. Therefore, the importance of oxygen sensing cannot be neglected. Identifying oxygen at ultra-low concentrations,[1] where the oxygen partial pressure (pO_2) is below 0.25 kPa, is significant in life science, given the minimum concentrations of oxygen required for tissue[2] and cell metabolism.[3] Ultra-low oxygen detection is also crucial in some industry fields, such as food packaging[4] and aviation.[5] Compared to conventional techniques, including Clark electrodes,[6] radioisotope,[7] and nuclear magnetic resonance,[8] luminescence-based oxygen sensing[9–11] has particular advantages of being non-invasive, nontoxic, rapid, and reversible.

Single-molecule spectroscopy[12–15] can remove ensemble averaging, revealing the dynamics at the nano-scale. It provides a promising alternative for oxygen sensors in the nano-environment with a high spatial resolution and sensitivity. By performing the fluorescence correlation spectroscopy of single Rhodamine molecules, it has been found that the triplet transition rate of single molecules was oxygen-sensitive and the sensitivity can be up to 0.1 kPa^{-1}.[16] Erker *et al.* have reported that the dissolved oxygen concentration could be determined by measuring the change of fluorescence intensity of single TAMRA-hemocyanin subunits.[17] However, single-molecule sensors based on luminescence intensity cannot accommodate the fluctuations in luminescence, reducing the sensitivity for the detection of ultra-low oxygen concentrations.

In this paper, we propose a method for the detection of ultra-low oxygen concentrations based on the fluorescence blinking dynamics of single molecules. We use the fraction of time spent in the off-state (R_{off}) as an indicator of fluorescence blinking dynamics and analyze it with respect to the change in the oxygen concentration.

Figure 1 shows the schematic diagram of a home-built laser scanning confocal microscope[18–21] for single-molecule fluorescence detection. Single molecules were excited by a pulsed laser (Toptica, FemtoFiber Pro) with a repetition frequency of 80 MHz and a central wavelength of 635 nm. The laser was circularly polarized by using the combination of a quarter-wave plate and a half-wave plate and then collimated by a beam expander. After passing through an excitation filter (Chroma, HQ620/60x), the laser beam was directed by a dichroic mirror (Chroma, Q660LP) and a fast steering mirror (Newport, FSM-300-M-03) toward an objective (Olympus, LUCPFLN60×, NA = 0.7) with an adjustable ring for glass window correction. The laser was focused onto the sample with a diameter of about 300 nm and an excitation energy of 0.5 pJ per pulse. A telecentric lens system was used

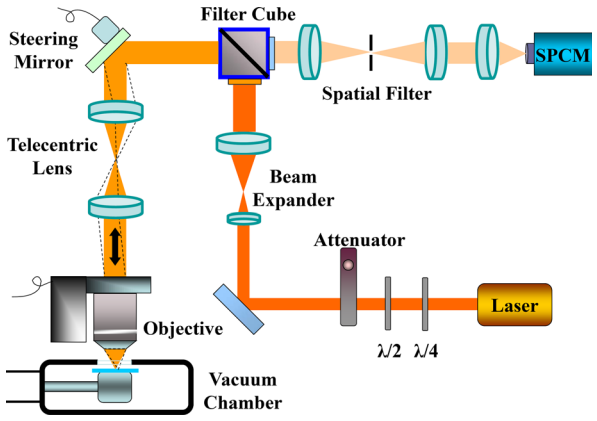

FIG. 1. Schematic of a laser scanning confocal microscope for single-molecule fluorescence detection.

a)E-mail: chenry@sxu.edu.cn
b)E-mail: xlt@sxu.edu.cn

between the steering mirror and the objective. Fluorescence imaging of single molecules was performed by scanning the incident angle of the laser beam, exciting the sample, and collecting the fluorescence point-by-point. The collected signal was then filtered by an emission filter (Chroma, ET655lp) and a notch filter (Chroma, ZET635nf). Fluorescence was then focused through a spatial filter of 100 μm and detected using a single-photon counting module (SPCM, PicoQuant, τ-SPAD-50, Germany).

The squaraine-derived rotaxane (SR, 1001, Molecular Targeting Technologies, Inc.) molecule belongs to the class of oxygen-sensitive ionic dyes.[22] Its chemical structure and spectral information can be found in Fig. S1 in the supplementary material. SR molecules were dissolved in Milli-Q water and diluted to a concentration of 10^{-10}–10^{-9} M. Here, the concentration was low enough to ensure that molecules were separated from each other and there was no more than one molecule appearing in the excitation spot. A diluted solution of 50 μl was spin-coated onto the glass substrate at a rate of 3000 rpm. The glass coverslips (Ted Pella, 260340) were cleaned previously by sonication in acetone, potassium hydroxide solution, and Milli-Q water and then irradiated under an ultraviolet lamp for 1 h. The single-molecule sample was mounted in a vacuum chamber where the oxygen concentration was varied by controlling the air pressure. In this experiment, pO_2 was adjustable from 20 to 0.01 kPa. A control experiment was also performed by purging the chamber with pure nitrogen gas several times and then refilling with nitrogen gas to 85 kPa (air pressure).

Figure 2 shows the typical fluorescence images of single SR molecules in varying environments. Figures 2(a)–2(c) demonstrate the fluorescence images of single molecules which were placed in three different oxygen atmospheres with the pO_2 of 20 kPa, 0.17 kPa, and 0.01 kPa, respectively. At the pO_2 of 20 kPa, single molecules have the highest fluorescence intensity level with the averaged fluorescence intensity of 9.6 kcps, as shown in Fig. 2(a). Along with the decrease in pO_2, the average fluorescence intensity decreases to 7.8 kcps at the pO_2 of 0.17 kPa in Fig. 2(b) and further to 4.7 kcps at 0.01 kPa in Fig. 2(c). Meanwhile, the pattern gradually deviates from a circle spot to an interrupted shape. Figure 2(d) shows a control experiment where single molecules are placed in a nitrogen environment with a pressure of 85 kPa, which presents similar results as Fig. 2(c). All these results indicate that the fluorescence properties of single molecules are sensitive to the oxygen concentration.

To reveal the underlying mechanism, we investigate the fluorescence trajectories of single molecules and compare the blinking dynamics accordingly. The corresponding fluorescence trajectories of single SR molecules are presented in Fig. 3. Identification of single molecules can be found in Fig. S7 in the supplementary material. From Fig. 3, we can see that the fluorescence blinking becomes more frequent as the oxygen concentration decreases. At the pO_2 of 20 kPa, single SR molecules show a strong and stable fluorescence intensity and only a few blinking behaviors are present, as shown in Fig. 3(a). In Fig. 3(b), at the pO_2 of 0.17 kPa, the fluorescence intensity decreases a little compared to that in Fig. 3(a). The blinking behavior becomes more pronounced, and the single molecules spend more time in the off-state. Finally, it can further change when the pO_2 decreases to 0.01 kPa, as shown in Fig. 3(c). Note that the 0.01 kPa pO_2 is basically close to an oxygen-free environment, and the fluorescence trajectory does not show any noticeable change when N_2 is filled as a control experiment in Fig. 3(d). The fluorescence properties of more single SR molecules can be found in Figs. S2 and S3 in the supplementary material.

The influence of the oxygen concentration on the fluorescence property of single molecules can be further revealed by analyzing their blinking dynamics. To analyze the fluorescence blinking dynamics of single molecules, a threshold intensity, distinguishing on- and off-state events from the fluorescence trajectory, is defined as three-fold standard deviations of background higher than the average background level, as indicated by the gray line in the fluorescence trajectory and intensity histogram in Fig. 4(a). The probability density $P(\tau_i)$ of the duration time for the on- or off-state events can be determined by the following definition:[23,24]

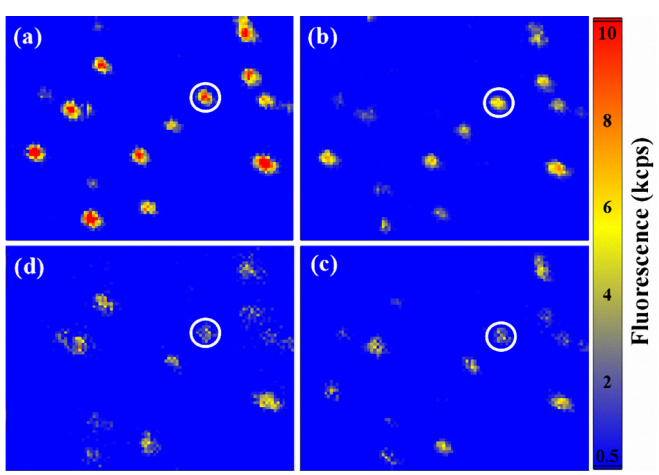

FIG. 2. Fluorescence images of single molecules for the same area (10 μm × 8 μm) at the oxygen partial pressure (pO_2) of (a) 20 kPa, (b) 0.17 kPa, (c) 0.01 kPa in air, and (d) the nitrogen condition with 85 kPa. The circle marks the same SR molecule in the four images.

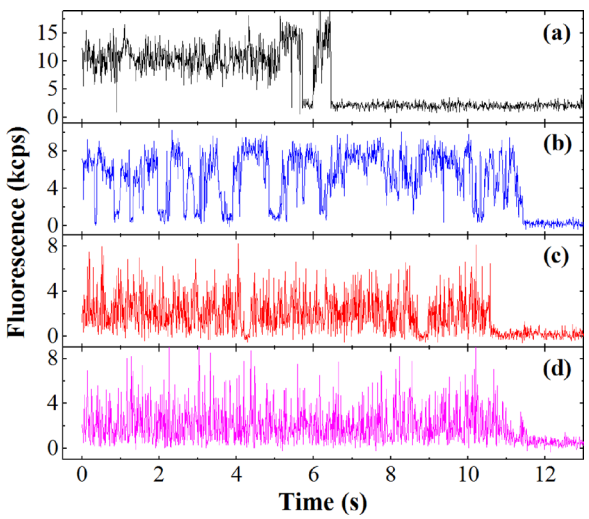

FIG. 3. Typical fluorescence trajectories of single molecules at the pO_2 of (a) 20 kPa, (b) 0.17 kPa, (c) 0.01 kPa in air, and (d) the nitrogen condition with 85 kPa, respectively. The integration time is 10 ms.

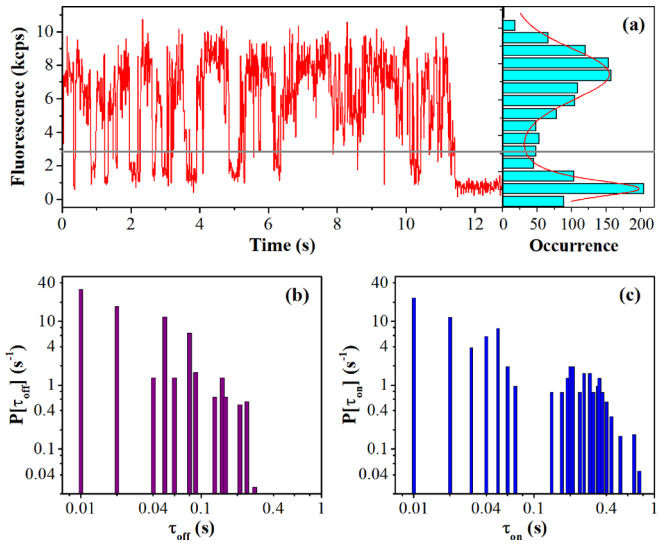

FIG. 4. The analysis of fluorescence blinking dynamics. (a) Fluorescence trajectory and intensity histogram of a typical single SR molecule at the pO_2 of 0.08 kPa. The gray line indicates the threshold intensity for identification of on- and off-state events. The distribution of probability density $P(\tau_i)$ for off- (b) or on-state (c) events is displayed in the log-log representation.

$$P(\tau_i) = \frac{N(\tau_i)}{N_{i,total}} \times \frac{1}{\Delta\tau_{i,av}} \ (i = \text{on or off}), \tag{1}$$

where $N(\tau_i)$ is the statistics of on- or off-state events in duration time τ_i, $N_{i,total}$ is the total number of on- or off-state events, and $\Delta\tau_{i,av}$ is the average of the time intervals to the preceding and following events. Figures 4(b) and 4(c) show the distribution of probability densities for off- and on-state events on double logarithmic coordinates, respectively.

The blinking dynamics can be characterized quantitatively by analyzing R_{off}, which represents the fraction of time spent in the off-state before photobleaching. R_{off} can be calculated through the following expression:

$$R_{off} = \frac{T_{off}}{T_{off} + T_{on}} = \frac{\sum P(\tau_{j,off}) \times \tau_{j,off}}{\sum P(\tau_{j,off}) \times \tau_{j,off} + \sum P(\tau_{j,on}) \times \tau_{j,on}}, \tag{2}$$

where T_{off} and T_{on} are the accumulative times for off- and on-state events of single molecules before fluorescence bleaching. R_{off} is 30.6% for the single molecule in Fig. 4(a) with the parameters ($T_{off} = 2.42$ s and $T_{on} = 5.49$ s) calculated from Figs. 4(b) and 4(c), respectively. Although the detection of duration time τ for the on- or off-state events can be influenced by the bin time of the experiment, it is found that R_{off} is unchanged, which can be observed in Figs. S4–S6 in the supplementary material, from where it is indicated that the value of R_{off} is independent of the time resolution.

We statistically analyzed R_{off} of about 100 single SR molecules under ten different conditions, as presented in Table I. We found that R_{off} of single molecules changes dramatically with the decrease in pO_2 in the range of 0.01–0.25 kPa. This makes it clear that R_{off} would be used as a sensitive indicator for oxygen detection. The relative change of R_{off} can be analysed in a Stern-Volmer plot[10] which is a plot of the relative value of the indicator versus oxygen concentration. By choosing R_{off} of single molecules in the nitrogen gas to be the initial amount R^0_{off}, we evaluated the relative values (R^0_{off}/R_{off}) at different oxygen concentrations, as shown in Fig. 5(a). The curve was fitted using a two-site quenching model[25]

$$\frac{R^0_{off}}{R_{off}} = A \times \left[\frac{f_1}{(1 + k_1 \times pO_2) \times \exp(m_1 \times pO_2)} + \frac{f_2}{(1 + k_2 \times pO_2) \times \exp(m_2 \times pO_2)} \right]^{-1}, \tag{3}$$

where f is the fractional contribution to each component with $f_1 + f_2 = 1$, k and m are the Stern-Volmer constant and exponential index of the corresponding oxygen accessible sites, respectively, and A is the correction term that is independent of the oxygen concentration. The Stern-Volmer plot for R_{off} fits well with a combination of the following values: $f_1 = 0.04$, $k_1 = 0$, $m_1 = 0$, $f_2 = 0.96$, $k_2 = 38.14$, and $m_2 = 7.09$.

To compare the oxygen sensing methods of fluorescence blinking and intensity, the oxygen sensitivity K, defined as the relative signal change per kPa oxygen, can be calculated using the following equation:[10]

$$K \equiv \lim_{pO_2 \to 0} \frac{1}{I} \left| \frac{\Delta I}{\Delta pO_2} \right| = f_1 \times (k_1 + m_1) + f_2 \times (k_2 + m_2). \tag{4}$$

There is a high oxygen sensitivity of 43.42 kPa^{-1}, especially in the ultra-low oxygen concentration (0.01–0.25 kPa pO_2).

The Stern-Volmer plot for fluorescence intensity of single SR molecules with respect to the oxygen concentration is also presented in Fig. 5(b). The fluorescence intensity of single molecules is quenched gradually with the oxygen concentration varying from 20 to 0.01 kPa pO_2. The experimental results can be fitted using a two-site quenching model in the Stern-Volmer plot with a combination of numerical values for all parameters: $f_1 = 0.52$, $k_1 = 0.01$, $m_1 = 0$, $f_2 = 0.48$, $k_2 = 0.03$, and $m_2 = 12.59$. The oxygen sensitivity from the fluorescence-intensity measurement is about 6.06 kPa^{-1}. Thus, the scheme based on fluorescence blinking analysis exhibits sensitivity around seven times higher, especially in the determination of the ultra-low oxygen concentration.

There exist two dark states (triplet state T_1 and radical cationic state R^+) which would affect the fluorescence property of single SR molecules.[26] Figure 6 shows the simplified energy-level scheme and electronic transition pathways for a

TABLE I. Statistic results of the most probable value and distribution of R_{off} under different pO_2 values.

	Air									N_2
pO_2 (kPa)	20	8.5	4	0.5	0.3	0.17	0.08	0.03	0.01	…
R_{off} (%)	3.0 ± 2.0	3.5 ± 2.2	3.2 ± 2.0	3.1 ± 1.9	4.0 ± 2.7	7.2 ± 5.1	9.8 ± 7.9	44.4 ± 14.4	54.3 ± 16.2	56.1 ± 15.3

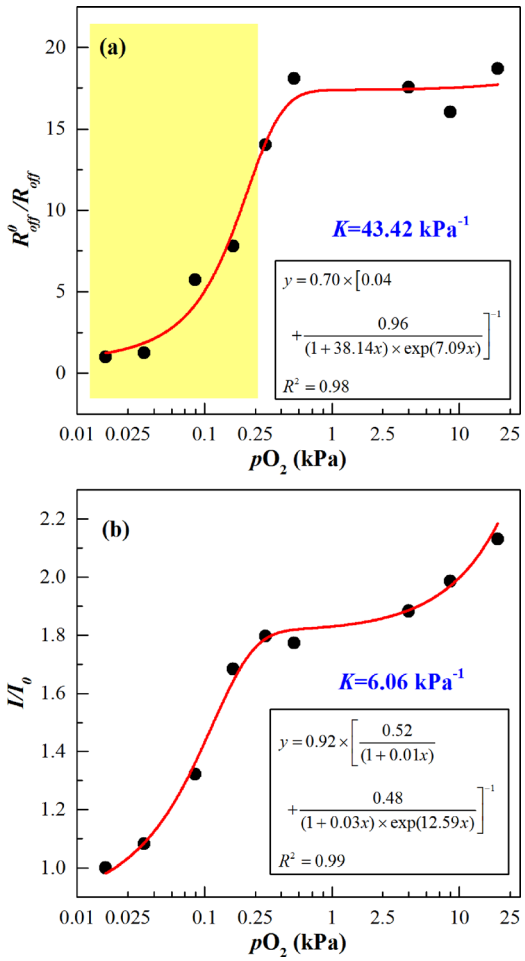

FIG. 5. Stern-Volmer plots on R_{off} of fluorescence blinking (a) and intensity (b) in the logarithmic coordinates for single SR molecules. The yellow highlighted area indicates high oxygen sensitivity in the range of 0.01–0.25 kPa pO_2.

single molecule. A single molecule in the ground state (S_0) can be excited to its first excited state (S_1) by absorbing a single photon. It can either return directly to S_0 through a radiative recombination to emit a photon (fluorescence) or transfer to T_1 via intersystem crossing.[27–29] T_1 has two depopulation channels, either relaxing from T_1 back to S_0 or transferring to a long-lived R^+, and then returning to S_0. Although T_1 plays an important role in blinking,[15] fluorescence blinking of single molecules cannot be explained by intersystem crossing to T_1 alone, especially those with long off-time durations.[30] The blinking with long off-time durations has been generally considered to be caused by long-lived radical ion states.[31,32] It has been reported that a non-fluorescent, radical cationic state (R^+) can be produced by electron transfer from a triplet fluorophore to molecular oxygen along with the production of a superoxide radical (O_2^-).[33]

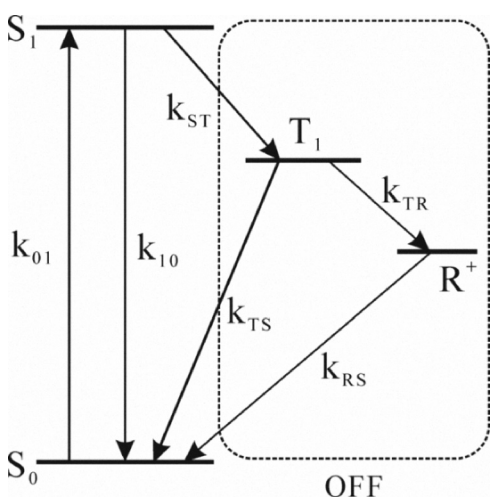

FIG. 6. Simplified energy-level scheme and electronic transition pathways for single molecules. Both the triplet state (T_1) and the radical cationic state (R^+) give rise to fluorescence blinking.

When pO_2 is high, we can see rare blinking events but with long off-time durations. The blinking with long off-time durations cannot be attributed to T_1 because T_1 has a short lifetime due to the fast decay induced by oxygen.[29,34] It has also been reported that the quenching rate of T_1 by molecular oxygen is faster than the formation of radical states, which leads to quite small probability of the formation of radical states in the presence of molecular oxygen.[33] However, when single molecules were prepared onto glass or in matrix films, rare blinking events with long off-time durations can always be found in air conditions,[31,35] as well as in our experiment, as shown in Fig. 3 and Figs. S2 and S3 in the supplementary material. It can be inferred that long-lived R^+ is a dominant dark state which brings about fewer fluorescence blinking events with long off-time durations at high pO_2. Therefore, R_{off} is small at high pO_2, as shown in Table I.

When pO_2 is low, more frequent fluorescence blinking events with short off-time durations can be found in the fluorescence trajectories, as shown in Fig. 3 and Figs. S2 and S3 in the supplementary material. The lifetime of the triplet state T_1 becomes longer in the absence of oxygen, as shown in Fig. S8 in the supplementary material. However, the lifetime of T_1 is still shorter than that of R^+. In addition, we can hardly observe the blinking events with long off-time durations in the fluorescence trajectory at low pO_2. Because the formation of R^+ is an oxygen assistant process,[33] it can be inferred that the formation of R^+ will be suppressed and T_1 becomes a dominant dark state for frequent fluorescence blinking with short off-time durations in the absence of oxygen. More blinking events not only result in larger R_{off} but also reduce the fluorescence intensity.[26]

In summary, we have presented a sensitive method for ultra-low oxygen concentration detection based on the fluorescence blinking dynamics of single SR molecules. The change in blinking behavior of single molecules at different oxygen concentrations can be attributed to the oxygen-dependent electron transfer dynamics of triplet and radical cationic states. Our method showed sensitivity around seven times greater than the fluorescence-intensity measurement of ultra-low oxygen concentrations in the range of 0.01–0.25 kPa pO_2. This oxygen-sensing scheme can be used to monitor ultra-low oxygen concentrations in life science and industry fields.

See supplementary material for additional information regarding the chemical structure and spectra of the squaraine-derived rotaxane (SR) molecule, more fluorescence trajectories of single SR molecules at different oxygen

partial pressures, fluorescence trajectories of single SR molecules with different bin times, methods for identification of single molecules, and dependence of triplet lifetime on the oxygen partial pressure. This material is available free of charge via the Internet at http://aip.scitation.org.

This work was supported by the National Key Research and Development Program of China (No. 2017YFA0304203), the National Natural Science Foundation of China (Nos. 61527824, 11504216, 11374196, 61675119, 11434007, 11404200, and U1510133), PCSIRT (No. IRT13076), 1331KSC, and the Applied Basic Research Program of Shanxi Province (No. 201601D021016).

[1]S. Medina-Rodriguez, M. Marin-Suarez, J. F. Fernández-Sánchez, A. de la Torre-Vega, E. Baranoff, and A. Fernández-Gutiérrez, Analyst **138**, 4607 (2013).
[2]E. Roussakis, Z. Li, A. J. Nichols, and C. L. Evans, Angew. Chem., Int. Ed. **54**, 8340 (2015).
[3]X. Zheng, H. Tang, C. Xie, J. Zhang, W. Wu, and X. Jiang, Angew. Chem., Int. Ed. **54**, 8094 (2015).
[4]R. S. Cruz, G. P. Camilloto, and A. C. d. S. Pires, in *Structure and Function of Food Engineering*, edited by A. A. Eissa (InTech, Rijeka, 2012), p. 21.
[5]F. Czerwinski, Corros. Sci. **86**, 1 (2014).
[6]Z. Wang, P. Lin, G. A. Baker, J. Stetter, and X. Zeng, Anal. Chem. **83**, 7066 (2011).
[7]M. Lubberink, Y. Y. Wong, P. G. Raijmakers, R. C. Schuit, G. Luurtsema, R. Boellaard, P. Knaapen, A. Vonk-Noordegraaf, and A. A. Lammertsma, J. Nucl. Med. **52**, 60 (2011).
[8]V. H. Liu, C. C. Vassiliou, S. M. Imaad, and M. J. Cima, Proc. Natl. Acad. Sci. U.S.A. **111**, 6588 (2014).
[9]X. D. Wang and O. S. Wolfbeis, Chem. Soc. Rev. **43**, 3666 (2014).
[10]S. Medina-Rodríguez, Á. de la Torre-Vega, C. Medina-Rodríguez, J. F. Fernández-Sánchez, and A. Fernández-Gutiérrez, Sens. Actuators, B **212**, 278 (2015).
[11]M. Quaranta, S. M. Borisov, and I. Klimant, Bioanal. Rev. **4**, 115 (2012).
[12]W. E. Moerner, Rev. Mod. Phys. **87**, 1183 (2015).
[13]H. Liu, Y. Fan, J. Wang, Z. Song, H. Shi, R. Han, Y. Sha, and Y. Jiang, Sci. Rep. **5**, 14879 (2015).
[14]X. Cai and Y. Zheng, Phys. Rev. A **95**, 052104 (2017).
[15]B. Kozankiewicz and M. Orrit, Chem. Soc. Rev. **43**, 1029 (2014).
[16]N. Opitz, P. J. Rothwell, B. Oeke, and P. Schwille, Sens. Actuators, B **96**, 460 (2003).
[17]W. Erker, S. Sdorra, and T. Basché, J. Am. Chem. Soc. **127**, 14532 (2005).
[18]R. Wu, R. Chen, C. Qin, Y. Gao, Z. Qiao, G. Zhang, L. Xiao, and S. Jia, Chem. Commun. **51**, 7368 (2015).
[19]Y. Gao, C. Qin, Z. Qiao, B. Wang, W. Li, G. Zhang, R. Chen, L. Xiao, and S. Jia, Appl. Phys. Lett. **106**, 131103 (2015).
[20]C. Qin, Y. Gao, Z. Qiao, L. Xiao, and S. Jia, Adv. Opt. Mater. **4**, 1429 (2016).
[21]H. Zhou, C. Qin, R. Chen, G. Zhang, L. Xiao, and S. Jia, Appl. Phys. Lett. **105**, 153301 (2014).
[22]J. J. Gassensmith, J. M. Baumes, and B. D. Smith, Chem. Commun. **2009**, 6329.
[23]M. Kuno, D. P. Fromm, H. F. Hamann, A. Gallagher, and D. J. Nesbitt, J. Chem. Phys. **115**, 1028 (2001).
[24]S. Y. Jin, N. H. Song, and T. Q. Lian, ACS Nano **4**, 1545 (2010).
[25]B. Valeur and M. N. Berberan-Santos, *Molecular Fluorescence: Principles and Applications*, 2nd ed. (Wiley-VCH, Weinheim, 2012).
[26]E. M. Stennett, M. A. Ciuba, and M. Levitus, Chem. Soc. Rev. **43**, 1057 (2014).
[27]J. H. van der Velde, J. Oelerich, J. Huang, J. H. Smit, A. A. Jazi, S. Galiani, K. Kolmakov, G. Guoridis, C. Eggeling, A. Herrmann, G. Roelfes, and T. Cordes, Nat. Commun. **7**, 10144 (2016).
[28]J. Veerman, M. Garcia-Parajo, L. Kuipers, and N. Van Hulst, Phys. Rev. Lett. **83**, 2155 (1999).
[29]C. G. Hübner, A. Renn, I. Renge, and U. P. Wild, J. Chem. Phys. **115**, 9619 (2001).
[30]A. Renn, J. Seelig, and V. Sandoghdar, Mol. Phys. **104**, 409 (2006).
[31]R. Zondervan, F. Kulzer, S. B. Orlinskii, and M. Orrit, J. Phys. Chem. A **107**, 6770 (2003).
[32]M. Haase, C. G. Hübner, E. Reuther, A. Herrmann, K. Müllen, and T. Basché, J. Phys. Chem. B **108**, 10445 (2004).
[33]Q. Zheng, M. F. Juette, S. Jockusch, M. R. Wasserman, Z. Zhou, R. B. Altman, and S. C. Blanchard, Chem. Soc. Rev. **43**, 1044 (2014).
[34]H. Piwoński, R. Kołos, A. Meixner, and J. Sepioł, Chem. Phys. Lett. **405**, 352 (2005).
[35]E. K. L. Yeow, S. M. Melnikov, T. D. M. Bell, F. C. De Schryver, and J. Hofkens, J. Phys. Chem. A **110**, 1726 (2006).